Detecting small-scale geological structures using diffraction attributes

Juhe Wang [1, 2, *], Xiuping Chen [1, 2], Mengcheng Shu [3], Sen Cheng [4]

[1] Petroleum Engineering Technology Research Institute, Sinopec Northwest Oilfield Company, Urumqi, China
[2] Key Laboratory of Enhanced Recovery for Fracture-Cave Oil Reservoir, Sinopec, Urumqi, China
[3] China University of Petroleum, Beijing, China
[4] Nanjing GeoButton Information Tech. Co., Ltd, Nanjing, China

Abstract. We developed a method that uses diffracted wave data to address the issue of precisely characterizing small geological structures in a reservoir and demonstrated its effectiveness using model calculations. The method was implemented to characterize a fractured reservoir and igneous rock intruded in a carbonate reservoir. Two diffraction attributes were analyzed to precisely characterize the fine, small-scale geological structures therein. Principal component analysis was performed to extract diffraction data from seismic wave fields, and the reflection and diffraction wave fields were separated based on the kinematics and dynamics of the diffracted waves. The resulting diffracted wave fields provided an excellent basis upon which to assess the distribution of small geological structures in the study area. This proved, experimentally, that our diffraction-based method has the potential to characterize the distribution of small geological structures precisely and holistically.

1. Introduction

With the intensification of oil and gas prospecting worldwide, the precise characterization of small- and medium-scale geological structures in reservoirs has become an important issue. The detection of fracture cavities in carbonate (Zhang, 2008; Qian, 2008) and fractured reservoirs (Murray, 1968; Ruger, 1997; Neves, 2004; Al-Dossary, 2004; Shen, 2002; Gray, 2000; Hall, 2003; Schoenberg, 1999) in particular, are the matters of particular interest in oilfield exploration. However, it is very difficult to characterize these types of geological structures using conventional seismic reflection methods, due mainly to their limitations in terms of wave field resolutions.

It has been demonstrated that diffracted wave fields can be readily utilized to characterize small geological structures (Gallop & Hron, 1998; Klem-Musatov, 2008; Taner, 2006; Zhu, 2010; Priezzhev et al., 2013). Diffracted wave fields extracted from seismic datasets are particularly useful for characterizing geological structures with dimensions similar to or smaller than the resolution of the seismic reflection data (that is, smaller than $\lambda/4$). Various diffraction wave separation methods have been proposed based on the dynamics and wave characteristics of the diffracted wave fields (Xie, 2021; Liang, 2019). Pre-stack diffraction separation methods are computationally inefficient; therefore, they are not suitable for the rapid identification of reservoir strata. Subsequently, post-stack diffraction imaging has become an important tool for detecting such strata. Therefore, we propose a method for separating diffracted waves from seismic wave fields in a way that considers the kinematics and dynamics of seismic wave fields and is based on principal component analysis (PCA). Furthermore, we propose different methods for analyzing the attributes of diffracted waves to address a variety of geological problems, thereby enabling precise characterization of small-scale geological structures.

2. Principal component analysis-based post-stack diffraction separation

Post-stack diffraction separation is typically performed by differentiating diffracted and reflected waves based on their post-stack or post-migration amplitudes and phases and then separating the information from that of the diffracted waves. In this study, PCA was performed for separate diffractions based on the kinematics and dynamics of diffracted waves in post-stack seismic data (Shu, 2014).

PCA can be performed to separate a target volume of data into orthogonal volumes and rank the contribution of each orthogonal dataset to the total variance of the target data volume. PCA can, essentially, be expressed as follows:

$$\Lambda = \Phi^{\mathrm{T}} C \Phi \tag{1}$$

where C is the covariance matrix of the multidimensional vector X (in this work, C is the three-dimensional (3D) autocorrelation function of the data volume), Φ is an eigenvector of C, and Λ is the eigenvalue matrix.

Equation (1) was modified to accommodate 3D data volumes as shown in Equation (2) below. This equation

* Corresponding author: wangjh3278.xbsj@Sinopec.com

can be used to calculate the orthogonal data volume corresponding to each eigenvector and separate the features from different wave fields, thereby enabling the characterization of geological structures of varying size.

$$O^r_{ijk} = \frac{\lambda^r}{MNL}\sum_{m=1}^{M}\sum_{n=1}^{N}\sum_{l=1}^{L}\tilde{S}^r_{mnl}\tilde{\Phi}^r_{mnl} \quad (2)$$

$$\tilde{S}^r_{mnl} = \frac{S^r_{mnl}-\mu}{\sigma} \quad (3)$$

In this equation, O^r_{ijk} provides the r-th orthogonal component of the computed matrix, which is centered at i, j, k; S^r_{mnl} and $\tilde{S}^r_{mnl}$ are the matrices computed before and after standardization; n, m, and l are the spatial coordinates of the offset matrix participating in the calculation; N, M, and L are the number of offset matrices in each direction; μ is the average amplitude of the sampling points in the computed matrix; σ is the standard deviation of the amplitude of the sampling points in the computed matrix; λ^r is the eigenvalue of the matrix; and $\tilde{\Phi}^r_{mnl}$ is the diagonal matrix of Φ^r_{mnl}.

3. Analysis of diffraction features

Lens models of varying lateral widths and thicknesses were constructed to test the ability of diffracted waves to resolve small anomalies. The model parameters included a P-wave velocity of 2 km/s, wavelet frequency of 25 Hz, and wavelength of 80 m. The lenses were placed at a depth of 1 km.

3.1 Spatial resolution of diffracted waves

In this section, we will discuss the ability of the diffracted waves to detect lenses with changing lateral widths.

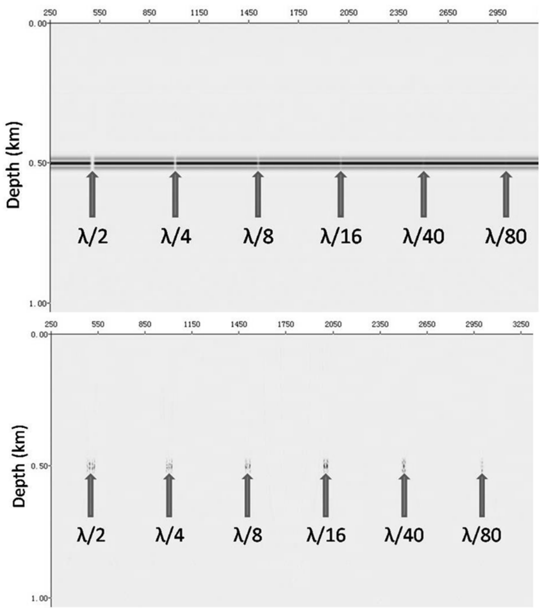

Fig. 2 (a) Forward model of lenses with different lateral widths. (b) Diffraction-derived data for lenses with different lateral widths

Figure 2 shows that the diffracted waves can detect and resolve the edges of lenses as narrow as λ/16 (5 m). Although lenses on the scale of λ/40 and λ/80 are very difficult to detect in seismic reflection offset profiles, the information derived from the diffracted waves can still be utilized to locate and characterize these very small lenses.

4. Examples of the characterization of small geological structures based on diffracted waves

4.1 Characterization of small igneous rock

This section describes the detection of small igneous rock intruded in a carbonate reservoir. In this example, the igneous rock are located at a depth of approximately 20 m from the top of the reservoir and interfere with the wave field. These igneous rock are usually very difficult to detect using conventional seismic reflection methods.
Diffraction information was extracted for the study area and the diffraction and reflection attributes were then compared. The well logs from Wells C, D, and E indicate that the structure and distribution of the reservoir were adequately characterized using the reflection Root Mean Square Amplitude (RMS) attributes (Fig. 3a). The extraction of stratigraphic attributes from the diffracted wave data (Fig. 3b) resulted in the diffracted wave field from the small igneous rock being highlighted as the former eliminated the seismic reflection features of the reservoir. As a result, the distribution of igneous rock encountered in Wells C and D were clearly characterized.

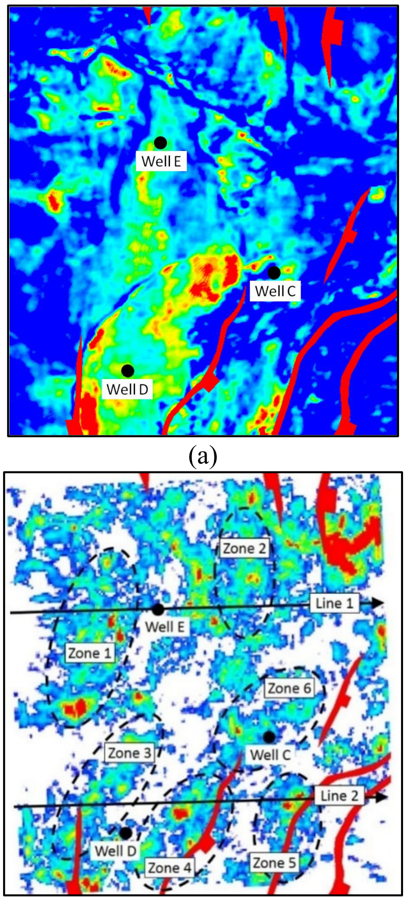

(b)

Fig. 3 RMS attribute map of the distribution of igneous rock in the study area.

RMS attributes of (a) the reflected waves and (b) the diffracted waves

3D seismic interpretation was conducted, based on the RMS attributes of the diffracted waves, for the continuous distribution of the diffracted wave energies. This allowed the 3D spatial distribution of the igneous rock present at Wells C and D to be obtained (Fig. 4).

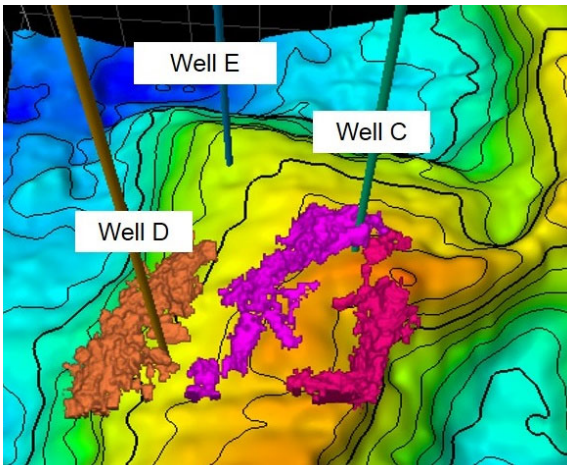

Fig. 4 Results of 3D seismic interpretation of igneous rock at Wells C and D

4.2 Characterization of small fracture systems

The distribution of fractures around a buried hilltop was characterized using RMS attributes derived from diffracted waves, as shown in Fig. 5, where the white sections represent areas with a high density of fractures. This result indicates that the fractures are located mainly on the sides of large, deep tectonic faults and are aligned nearly parallel to these. This result is consistent with that of the fractures revealed at Wells A and B.

The fracture spaces were also extracted from the diffracted wave data volume using the ant tracking method. The predicted fracture azimuths are presented in Fig. 6. Based on comparisons of data from Wells A and B, the predicted fracture azimuths from the diffracted wave data provide an excellent basis for assessing the overall distribution of fracture trends (green solid lines in Fig. 6) in the study area. The predictions are also consistent with the distribution of fractures detected at the wellbores, with the red dotted lines in Fig. 6 indicating the directions thereof.

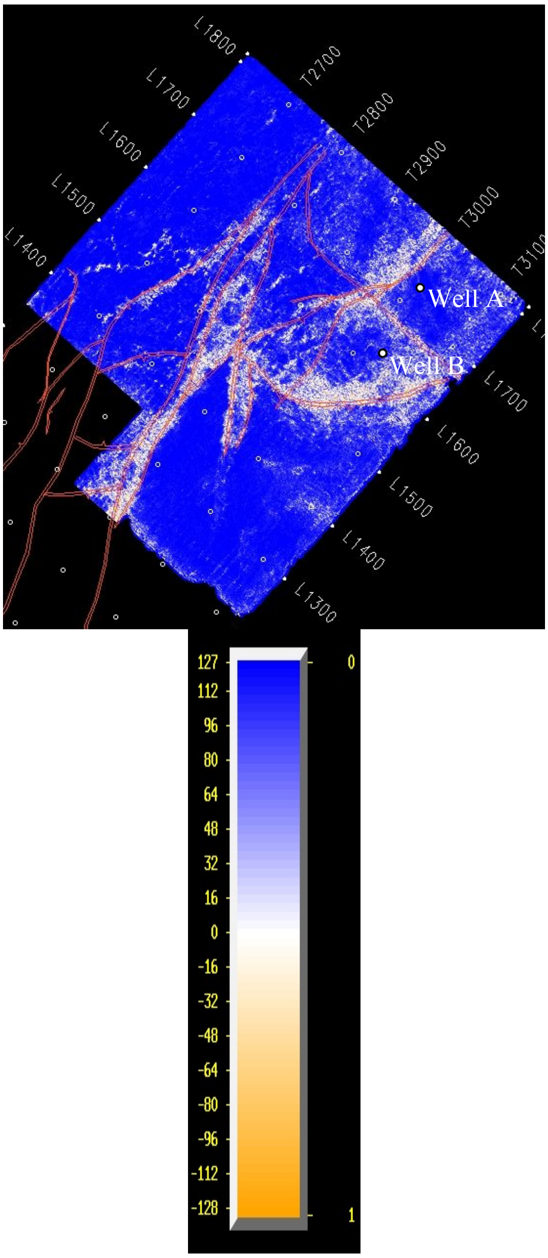

Fig. 5 RMS attribute map derived from the diffraction data volume

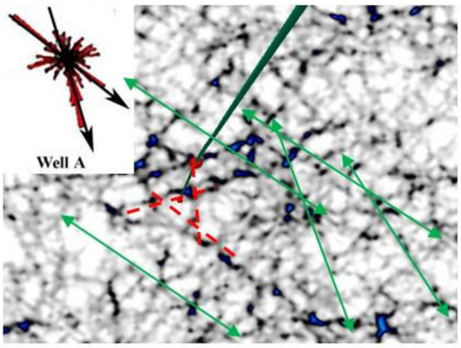

(a)

https://doi.org/10.1051/e3sconf/202235201074

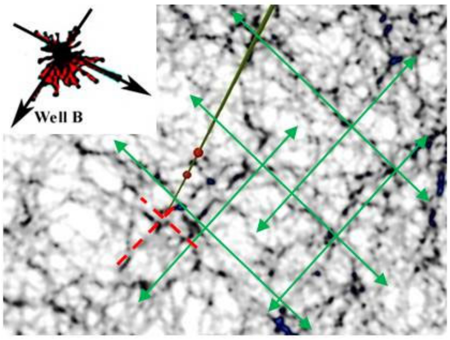

(b)

Fig. 6 Comparison between the diffracted predicted fracture azimuths and imaging logs for (a) Well A and (b) Well B

5. Conclusions

In this study, we presented a method for post-stack diffraction separation. Based on a forward modeled diffracted wave model, it was proven that this method can resolve geological structures as small as λ/40.
To detect the fractures in a fractured reservoir, we proposed a method based on the extraction of diffraction attributes from seismic data. The distribution of fracture densities in the study area and corresponding fracture azimuths were successfully predicted using our method and the predictions were validated using the well log data.
To detect igneous rock in a carbonate reservoir, we studied the separation of diffracted wave fields from igneous rock for which we proposed a method to predict the distribution of igneous rock. This method was successfully implemented to predict the spatial distribution of igneous rock within a well-controlled area and the predictions were validated using the well log data.

References

1. S. Al-Dossary, Y. Simon, and K. J. Marfurt, “Inter azimuth coherence attribute for fracture detection,” SEG Technical Program Expanded Abstracts, 23:183-186, 2004.
2. J. B. Gallop, and F. Hron, “Diffractions and boundary conditions in asymptotic ray theory,” Geophysical Journal International, vol. 133, no. 2, pp. 413-418, 1998.
3. D. Gray, “Head Kim Fracture detection in Manderson Field: A 3-D AVAZ case history,” Leading Edge, vol. 19, no. 11, pp. 1214-1221, 2000.
4. S. A. Hall, and J. M. Kendall, “Fracture characterization at Valhall: Application of P-wave amplitude variation with offset and azimuth (AVOA) analysis to a 3D ocean-bottom data set,” Geophysics, vol. 68, no. 10, pp. 1150-1160, 2003.
5. P Ivan, and S Aaron, “Fracture detection through seismic cube orthogonal decomposition,” SEG Annual Meeting, pp. 1308-1313, 2013.
6. K. D. Klem-Musatov, and A. M. Aizenberg, “Edge and tip diffractions theory and applications in seismic prospecting,” SEG 2008.
7. G. H. Murray, “Quantitative fracture study: Samish pool, Mckenzie County, North Dakota,” AAPG Bulletin, vol. 52, no. 1, pp. 57-65,1968.
8. F A Neves, M S Zahrani, S W. Bremkamp, “Detection of potential fractures and small faults using seismic attributes,” TLE, vol. 23, no. 9, pp. 903-906, 2004.
9. Ruger, “P-wave reflection coefficients for transversely isotropic models with vertical and horizontal axis of symmetry,” Geophysics, vol. 62, no.3, pp. 713-722, 1997.
10. M. A. Schoenberg, S. Dean, and C. M. Sayers, “Azimuth-dependent Tuning of seismic wave reflected from Fracture Reservoirs,” Geophysics, vol. 64, no. 4, pp. 1160-1171, 1999.
11. F. Shen, J. Sierra, D. Burns, M. N. Toksoz, “Azimuthal offset-dependent attributes (AVO AND FVO) applied to fracture detection,” SEG, Technical Program Expanded Abstracts, vol. 18, no. 1, pp. 776-785, 1999.